



Crustal Structure of Java, Indonesia, from Ambient Noise Tomography: Implications for Regional Tectonics

Iskandarsyah^{1,2}, Andri Dian Nugraha^{3,4}, Zulfakriza Zulfakriza^{3,4}, Irwan Meilano^{4,5}, Bayu Pranata⁶, Samsul Hadi Wiyono⁶, Aditya Lesmana⁷, Rexha Verdhora Ry³, Muzli Muzli⁶, Sesar Prabu Dwi Sriyanto⁶, Nova Heryandoko⁶

¹Earth Sciences Graduate Program, Faculty of Earth Sciences and Technology, Institut Teknologi Bandung, Bandung Indonesia, 40132

²Faculty of Faculty of Mathematics and Natural Sciences, Universitas Indonesia

³Global Geophysics Research Group, Faculty of Mining and Petroleum Engineering, Institut Teknologi Bandung, Bandung Indonesia, 40132

⁴Research Center of Disaster Mitigation, Institut Teknologi Bandung, Bandung Indonesia, 40132

⁵Faculty of Earth Science and Technology, Institut Teknologi Bandung, Bandung Indonesia, 40132

⁶Indonesian Meteorological, Climatological, and Geophysical Agency, Jakarta Indonesia.

⁷Geophysical Engineering Graduate Program, Faculty of Mining and Petroleum Engineering, Institut Teknologi Bandung, Bandung Indonesia, 40132

Correspondence to: Iskandarsyah (32421301@mahasiswa.itb.ac.id)

Abstract. Although local scale investigation throughout parts of the java island has been conducted to understand about the subsurface condition, there are only a few tomography approaches to prove the previews geological model. In this study we perform ambient noise tomography (ANT) of entire Java Island to delineate subsurface and the relationship between shear wave velocity and basin structure in relation to tectonic influences. Our study utilize data from 114 permanent seismograph stations operated by The Indonesian Meteorological, Climatological, and Geophysical, and Geophysical Agency (BMKG) of continuous seismic record from January-June 2022 (6 month). We obtain more than 6000 potentials of Empirical Green's function and extract the Rayleigh Group Velocity for the period 3s to 33s. We perform manual pick for dispersion curves of 6328 of pair cross correlation to correct any artefact. The two step tomography process begins with group wave velocity maps, then we delineate the shear wave velocity structure beneath Java Island from 3 to 30 km from 217 sampling point 1D inversion. Profile Vs ranges from 1.3 - 4.1 ±0.1 km/s with low Vs (1.3 - 2.2 ±0.1 km/s) interpreted as basins including Bogor, Kendeng and Banyumas basins. On the other hand, the high Vs (2.2 - 4.1 ±0.1 km/s) interpreted as crystalline basement or indicate stronger more rigid materials within the crust. The flexural pattern reveals a distinctive characteristic along Java Island, where the basin orientation shows regional variation. In western Java, the flexure trend indicates northward basin development, whereas in eastern Java the flexural axis shifts southward. In central Java, the transition between these two domains suggests a twisting or rotational deformation of the crust, reflecting a complex mechanical response of the Sunda Block to ongoing subduction processes beneath Java.



1 Introduction

Understanding the subsurface **profile** of Java Island is crucial in assessing geological hazards, exploring **nature** resources potential and advancing the knowledge of regional tectonic processes. The complex interplay between the **subduction** Indo-Australian Plate the overriding Eurasian Plate (Figure 1), and the associated volcanic arc has created
40 a heterogeneous lithospheric structure characterized by variations in crustal thickness, composition and seismic velocities (Widiyantoro et al., 2011). Recent advances in geophysical imaging techniques have significantly improved our ability to probe to these features. Among these, **ambient noise tomography** has emerged as a tool to image the upper crustal without the need for large earthquake datasets. By cross-**correlation** continues seismic noise recordings from multiple stations, this method reconstructs empirical Green's functions and retrieves surface wave dispersion
45 information that reflects subsurface structure (Bensen et al., 2007; Shapiro et al., 2005).

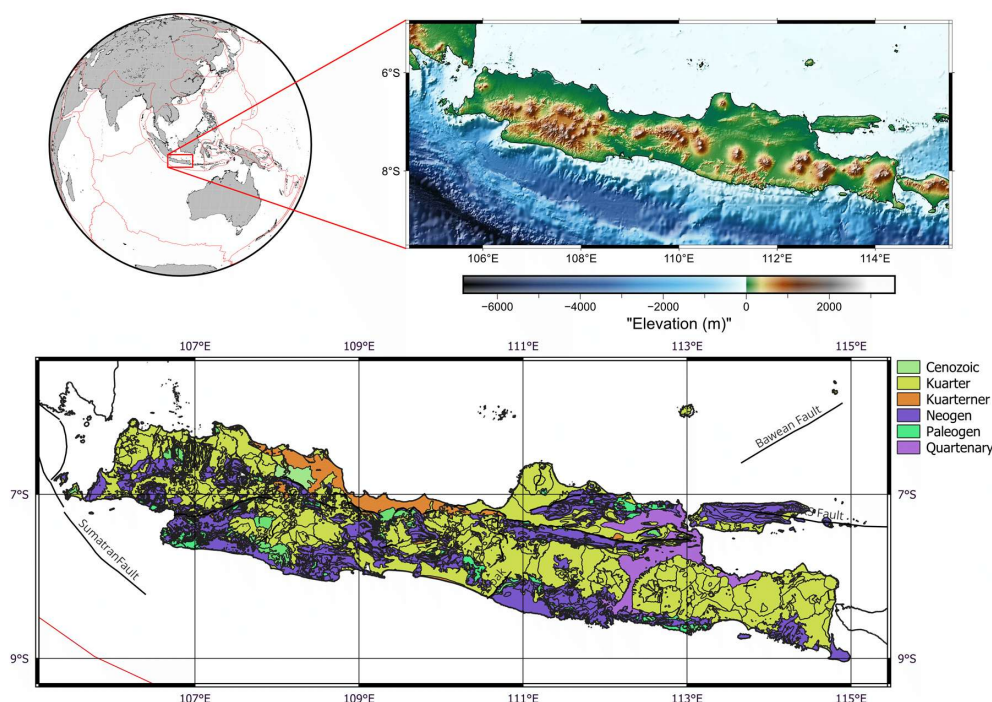


Figure 1: Location of area study, with elevation maps and modified geological map of Java Island Indonesia (Sigit, 1965; Steinshouer et al., 1999).

50 Based on previous studies, hypotheses regarding the subsurface condition of Java Island indicate significant variations in seismic wave velocities at various depths, particularly beneath the volcanic arc (Koulakov et al., 2007a; Wagner et al., 2007; Ramdhan et al., 2019; Muttaqy et al., 2022; Lesmana et al., 2025). Seismic tomography studies revealed low-velocity anomalies beneath the volcanic arc (Koulakov et al., 2007b), which are associated with the presence of hot mantle material resulting from the subduction process. Additionally, inversion of **seismic** wave data has shown



55 variation in shear wave velocity (V_s) that reflect differences in rock composition and temperature at intermediate to greater depths. Another hypothesis suggests the presence of weak zones Java that may serve as pathways for magma ascent, thereby enhancing volcanic activity along the volcanic arc (Widiyantoro et al., 2011). These studies provide critical insights into subsurface dynamics and potential geological hazards in the Java region.

60 From a geological perspective, one intriguing hypothesis regarding the subsurface conditions of Java Island is the existence of subduction process in the Earth's crust that enable mode dynamics interactions between the mantle and the upper crust (Noda, 2016). This process creates geological features for instance active faults, such as the Cimandiri Fault in West Java, the Opak Fault in Central Java, and the Kendeng Fault Zone extending into East Java (Irsyam et al., 2020), and the subduction-related deformation has contributed to the creation of major basins, including the North
65 Java Basin and the Kendeng Basin (Doust and Noble, 2008), which act as forearc and backarc depressions respectively. The present of this condition has yet to be fully supported by seismological evidence that interconnected to the entire of Java Island. Further studies using geophysical methods, such as ambient noise tomography, are needed to validate this hypothesis.

70 Despite significant advances in understanding Java's subsurface structure though the seismic tomography, existing studies remain fragmented in spatial coverage, resolution and integration. The pioneering work of ambient noise tomography at Java (Zulfakriza et al., 2013; Martha et al., 2017; Rosalia et al., 2022) has beneficial revealed of localized feature such as magma reservoir, sedimentary basins and fault zones at portion of regional scale. Furthermore, the specific research area in Java region (Pranata et al., 2020; Ry et al., 2023; Lesmana et al., 2025; Setiadi et al., 2025;
75 Syaifuddin et al., 2025) creates more disparities in resolution lead to incoherent structure comparisons. However, the regional or more connected interpretation of subsurface features would be complete and continue if the study generated through the entire island. Our study is bridging these methodological and special gaps to reveal Shear Wave velocity model and ultimately enhancing the understanding of the conceptual geology model (Husein, 2015; Aribowo et al., 2022).

80

The previous seismic tomography studies in Java region such as Bandung basin (Pranata et al. 2020), Banyumas basin (Setiawan et al. 2021), Jakarta basin (Saygin et al 2016; Ry et al. 2023) and Merapi volcano (Yudistira et al 2021) focused on specific volcanic or fault zones and not yet encompassing the entire island of Java. In this study, we investigate the crustal structure and tectonic implication in the Java region by using the ambient seismic noise cross
85 correlation. A regional sub surface profile of Java region is essential to provide a comprehensive mapping that correspond to geological structures, such as volcanic arcs, and major faults.

2 Data

We used continuous seismic data waveform of 114 seismic stations that operated by Indonesian Meteorological, Climatology and Geophysical Agency (BMKG) (see Figure 2). The recording instruments employed at these stations



90 have varying sampling rates, including 0.05 s, 0.025 s, and 0.02 s, depending on the type and model of the sensor. The distribution of seismic stations covered Southern Sumatra, Java, Madura and Bali Island. We use the seismic data waveform from January to July 2022 (6 months continue recording). We extract the Rayleigh wave from vertical component that retrieved from the cross-correlation of station pair. There are 6441 potential seismic station to cross correlate with range of distances about 4.16 km to 1531.43 km. We reduce the sampling rate to 0.2 s and applied the instrument correction and trend correction.

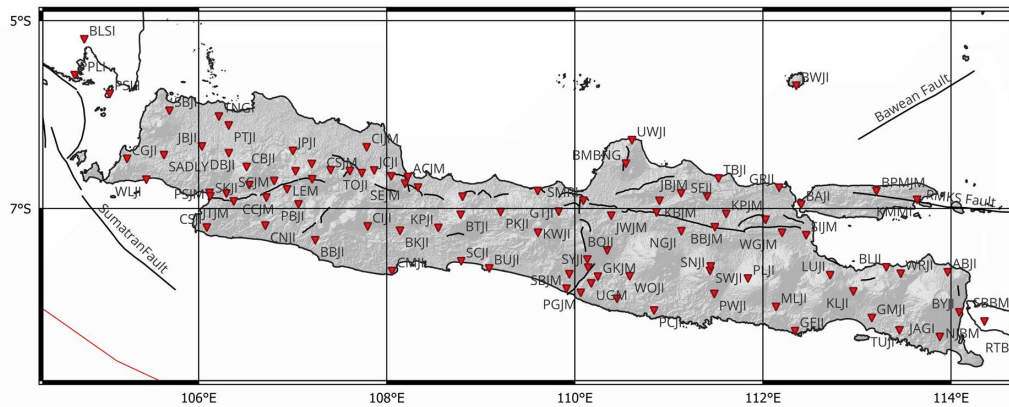


Figure 2: Distribution map of permanent broadband seismometers (BMKG seismographs network) across Java Island used in this study (Red inverted triangles) labeled with stations code. Black lines represent active fault systems in the region (Irsyam et al., 2020). The inset map provides the regional context of the study area within Indonesia.

100 3 Methods

3.1 ANT cross correlation

We apply the cross-correlation technique utilizes natural source such as wind, ocean waves, or human activities as a source of energy (Hennino et al., 2001). Cross correlation of seismic noise data recorded from seismographs at the seismic station to reconstruct the Green's function for information of seismic wave velocity structures between station (Shapiro et al., 2005). ANT method is highly beneficial in geophysical research due to its relatively low cost and its ability to deliver high-resolution subsurface image. Advances in technology and theoretical understanding of interferometry have further expanded the application of ambient noise, ranging from shallow exploration studies of earth crustal structures (Bensen et al., 2007).

105 the cross-correlation process is performed by transforming the time domain into the frequency domain using Fourier transformation, aiming to accelerate the computational process (Lewis, 1995).

The process of conversion of time domain to frequency domain also proven to be the fast and reliable course for cross correlation (Varotsos and Sarlis, 2024). Cross correlation executed by comparing seismic noise recording from two different locations and measuring the similarity of the recorded waves. Through this process, the travel time of seismic wave between the station can be estimated which is then used to map the surface structures (Campillo and Paul, 2003).

115 The Green's Function approximated through cross-correlation between two stations as time function of velocity propagation from one station to the other. Furthermore, the group velocity is measured by analyzing the arrival time



of dispersed waves at various frequency, particularly Rayleigh waves. Mapping the group velocity can be correlated to changes of subsurface materials elastic properties (Yang et al., 2007).

Several limitations applied to remove biases on the process. The first limitation is raypath must be more than 1.5
120 lambda on each period. Then every CC stack must have SNR more than 4 by comparing the peak amplitude with the rms noise (Tian and Ritzwoller, 2015). The last is the process of selecting the maximum energy of dispersion curves manually to remove any artefact effect of multiple wave package displayed in the dispersion curves. By applying this process, we can produce reliable travel time to compute 2-D group velocity and generate maps. After applying all the limitations, we inspected the raypath density coverage to ensure that the entire island of Java is effectively covered
125 (Figure 3).

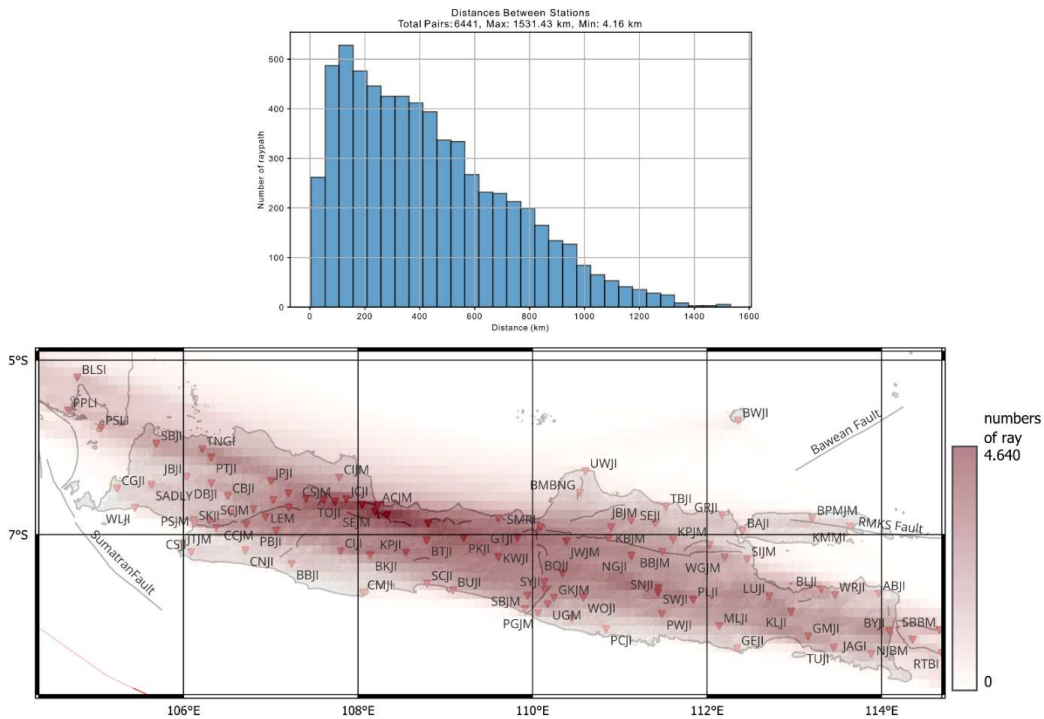
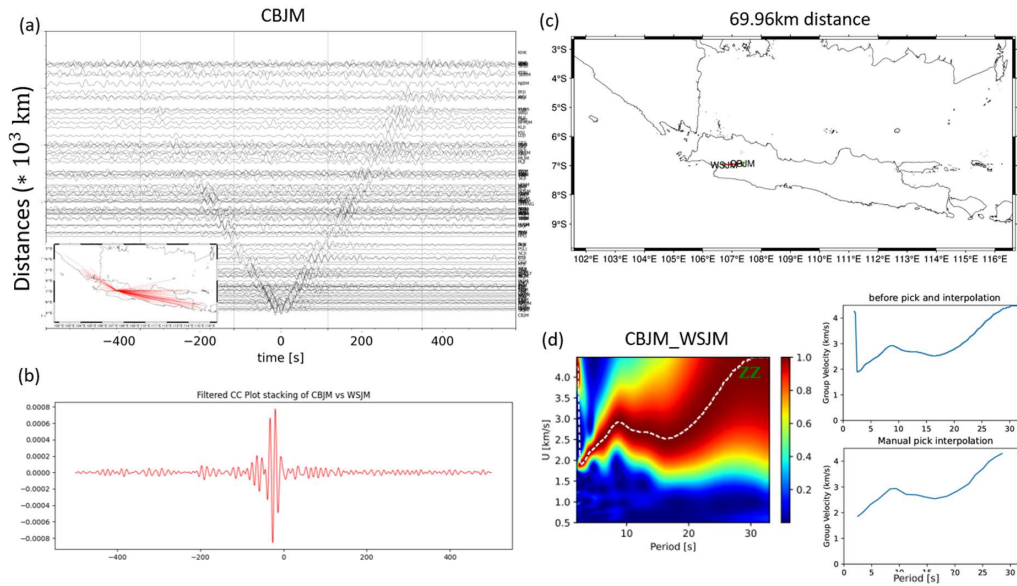


Figure 3: (Above) Statistic of raypath distance distribution of all station pairs in the study area (Java Island). (Below) Raypath distribution density indicated by low density (blue) to high density (red).

130 The cross-correlation outcome is high energy detected on the negative and/or positive delay time. Stacked of all stations with one reference station with distance can result in the continuity of delay time that form V shape (Figure 4 a). This procedure is significant to demonstrate the shape of distance over group velocity and visual quality data check.



135 **Figure 4: (a) The V shape of 6 months CCFs stacking in periode 3-33s of station CBJM with others. (b) CC of Station CBJM with WSJM showed time lag at negatif 30s. (c) Maps of CBJM and WSJM with distance of 69.96 km. (d) The dispersion curves of CBJM and WSJM with before and after manual pick.**

The dispersion curves process produces data of group velocity from period 3s to 33s. However, automatic picking from Noisy module (Jiang and Denolle, 2020) hold artefact value from different wave package (Figure 4 d). To solve this problem, we apply manual picking of 6821 curve dispersion to remove the artefact. The Dispersion curves show artefacts mostly appear at period less than 10 s indicated by high velocity jumps up to 4 Km/s, which rarely appears at low period.

140

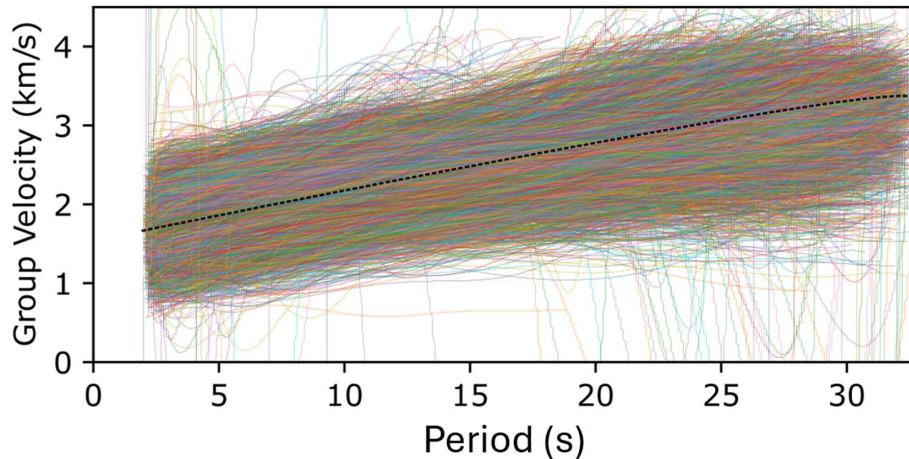


Figure 5: Dispersion curves from 6,821 manually selected measurements of group velocity. Each colored line represents an individual dispersion path, while the black dotted line shows the average group velocity at each period, fitted using a third-order polynomial.



145 2.2 Group velocity Modeling

The group velocity inversion is derived from frequency time analysis of cross correlation result. Frequency time analysis process applied in this study is Multiple Filter Analysis (MFA) (Dziewonski et al., 1969). The MFA construct estimated Rayleigh wave travel time at various frequencies. Additionally, the travel time is then interpreted into group velocities by considering the distance between stations. Group velocity dispersion curves from different periods
150 inverted using tomography methods to develop subsurface seismic velocity models. The covered periods of our result ranging from 3 to 33 seconds. The inversion process to map horizontal seismic group velocity operated using software FMST (Fast Marching Surface Tomography) (Rawlinson, 2005).

2.2 Shear wave modeling

The shear wave velocity (V_s) computed from seismic group velocity. The process begins with converting group velocity to phase velocity and then inverting the phase velocity curve to 1D V_s in depth domain (km) based on reference model. The selected point of pseudo dispersion curves in study area consists of 271 grid points with distance of 10 km each (Figure 6). The reference model based on AK135 (Kennett et al., 1995) as seismic velocity global standard model reference. The AK135 model provides initial distributions of P and S-wave velocity (V_p , V_s), and density at various depths. The inversion process involves matching the measured group velocity dispersion curve data
160 with the predicted dispersion curve from the theoretical model. During the inversion, the V_s parameter is adjusted iteratively until the simulated dispersion curve aligns with the observed data (Figure 7).

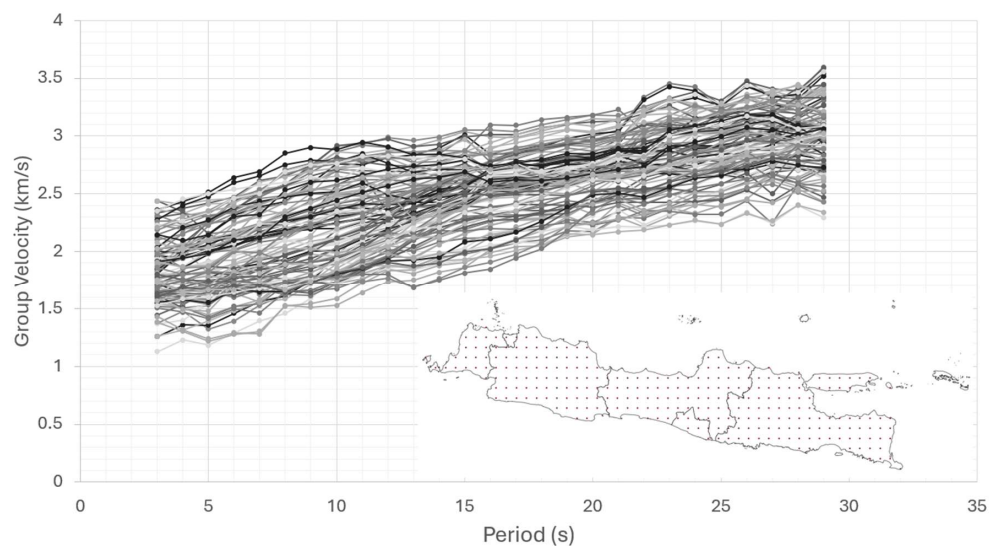
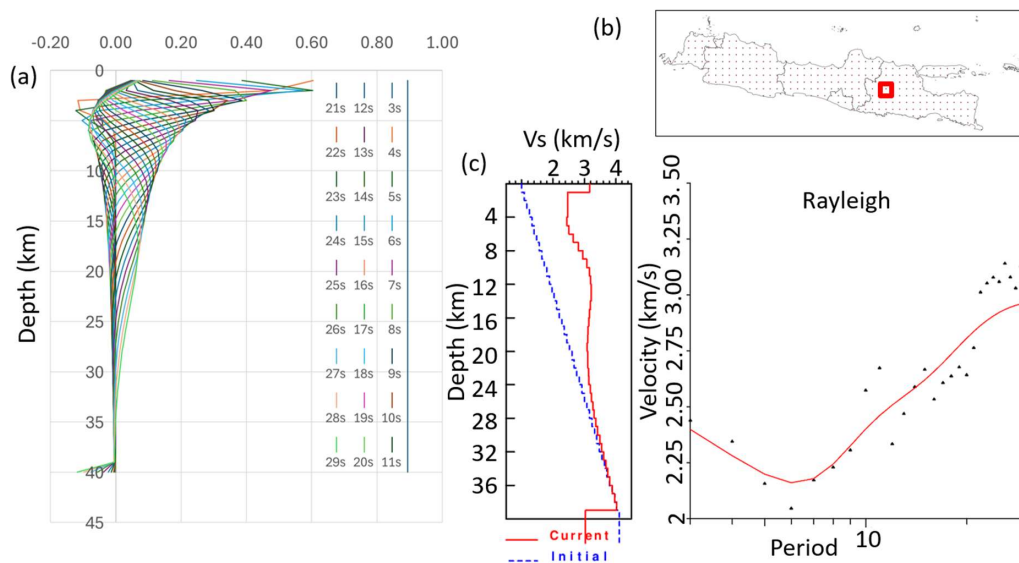


Figure 6: The pseudo-dispersion curves at 271 selected gridpoints (red dots in inset map) obtained from Rayleigh wave group velocity maps as spatial sampling point to be used for 1D V_s inversion.



165

Figure 7: Sensitivity kernel representative of point at the location (b). (b) Location of 1-D group velocity examples. (c) Inverted of group velocity (right) vs Period (s) to Shear wave velocity 'Vs' (left) with velocity model reference as initial model (blue line).

3 Result and Discussion

170 3.1 Checkerboard Resolution Test

We conducted the checkerboard resolution test to evaluate the ability of inversion method toward different grid sizes. We find that $0.5^0 \times 0.5^0$ grid size is the smallest grid possible that showing the best recovery result without smearing. The recovery checkerboard pattern remains clear without significant distortion or excessive smoothing (Figure 8). These results show that the model can distinguish lateral velocity variation for optimal seismic tomography study in

175 this area.

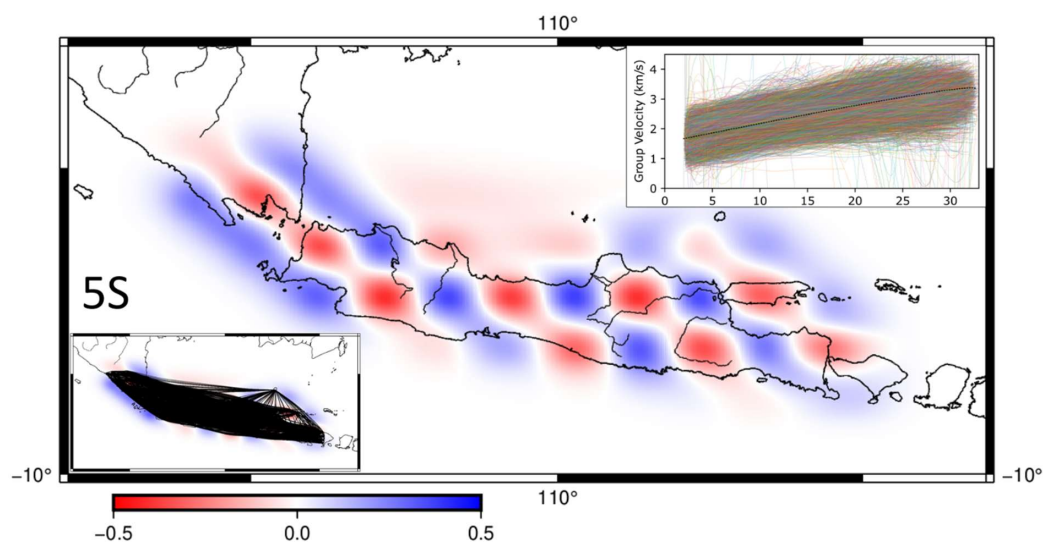
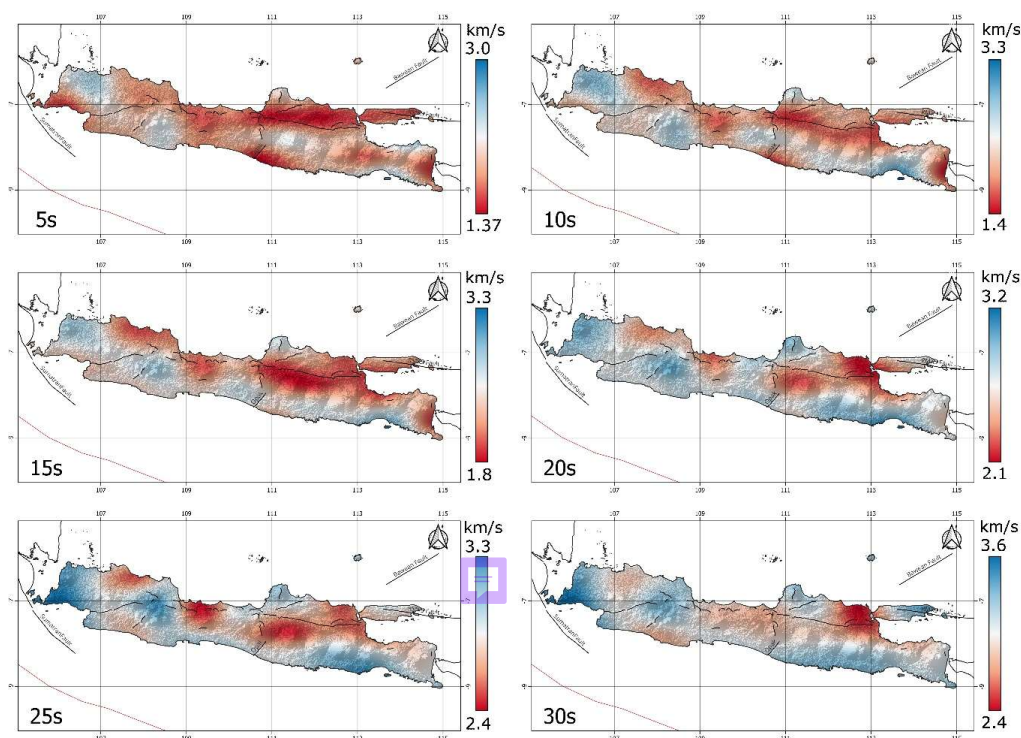


Figure 8: Recovery result of checkerboard at 5s period using grid size $0.5^{\circ} \times 0.5^{\circ}$. (bottom left) raypath coverage, (top right) dispersion curves.

3.2 Rayleigh Group Velocity Maps

180 Rayleigh group velocity maps of our study able to reveal information from period 3s to 33s that are consistent with the geological condition of Java Island (Figure 9). We divided the range into two sections, short (3-10s) and long (10-33s) period. The short period is associated with basins field with sedimentary sequence and the presence of volcanic activity. Furthermore, lower group velocities are detected along Java's main volcanic arc, reflecting the presence of volcanic materials and weaker, sedimentary layers near the surface. Conversely, higher group velocities are observed
185 in the northern and southern coastal areas, indicating harder and more stable bedrock outside the volcanic arc. In the longer periods (10–33 seconds), group velocities increase, reflecting deeper wave penetration into the Earth's crust, which correlates with basement crystalline as high velocity anomaly. This distribution of group velocities generally aligns with Java's regional geological model, where the volcanic arc, sedimentary basins, and subduction zone create measurable velocity variations across the island.



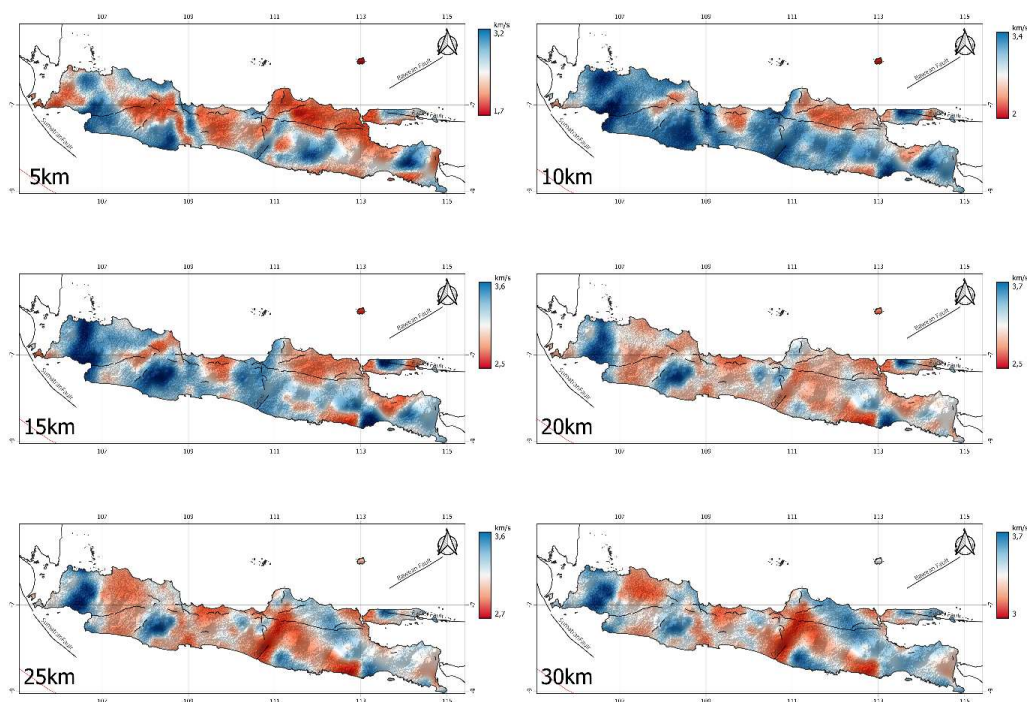
190

Figure 9: Group velocity lateral distribution across Java Island from period 5 to 30s.

3.3 Shear Wave Velocity Maps and Model

We construct shear wave velocity maps from combining 1D Vs for lateral distribution of tomography. The inversion successfully produces a shear wave velocity model from depths 3km to 29 km, corresponding to optimal resolution based on the sensitivity kernel of Rayleigh waves. The inversion result reveals significant shear wave velocity variation at different depths, reflecting subsurface structural changes. In one hand, the low velocity (1.4-2.2 km/s) at depth 5km suggest the existence of basins such Bogor, Banyumas and Kendeng Basins at the north of the back arc extension process (Figure 10). On the other hand, the high velocity (2.2-3.2 km/s) at similar depth explained of uplifted volcanic arc from compression process resulting more rigid igneous and/or metamorphic rocks.

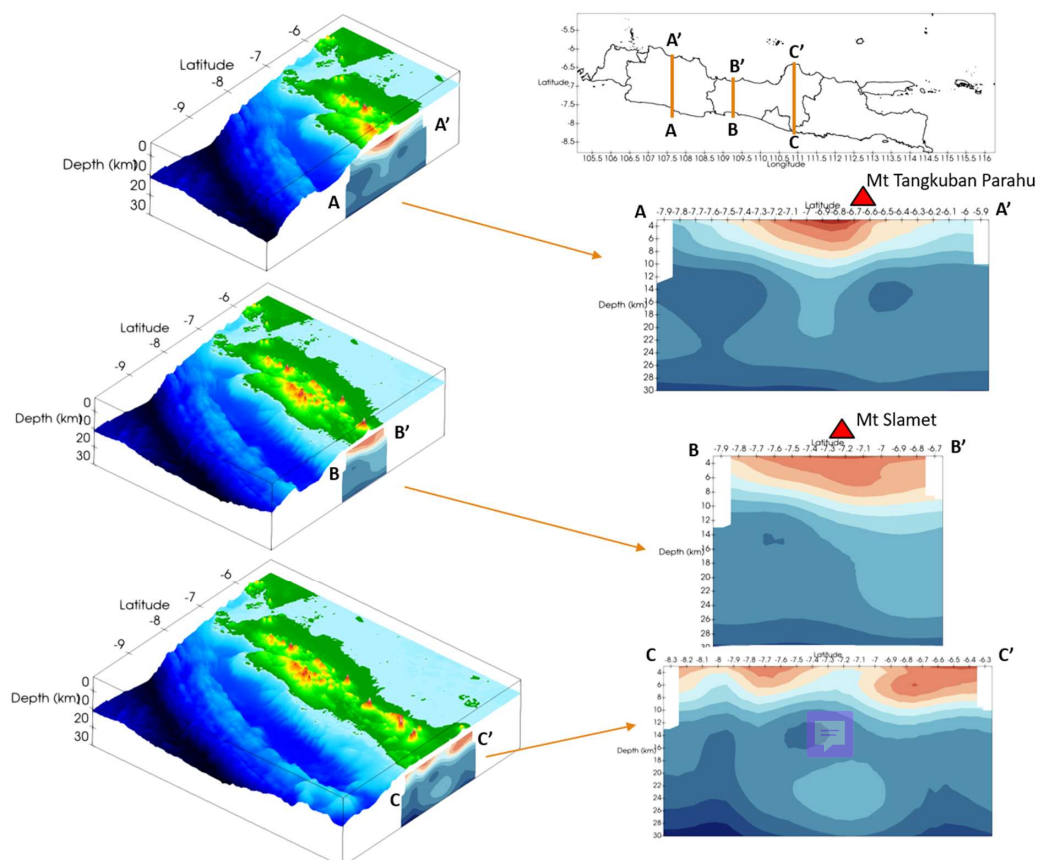
195



200

Figure 10: Horizontal view Vs structure Java Island at depths 5 -30 km. The blue and red color indicate high and low value Vs.

Three vertical profiles derived from the Vs 3D model of Java Island were constructed to visualize and interpret the subsurface structure (Figure 11). The west part represents the existence of Bogor basin at the north of Mount
205 Tangkuban Parahu. Similarly, the central region illustrates the Banyumas basin interpreted from low velocity value (1.7-2.2 km/s). Furthermore, the east region interpreted as Kendeng basin reveals a southward flexure of the sedimentary layers, indicating downward bending of the crust toward the volcanic arc.



210 **Figure 11: Vertical section of Vs passing through West (A-A'), Central (B-B') and East (C-C') Java regions. The blue and red color indicate high and low Vs value, respectively.**

Our ambient noise tomography result reveals the shear wave velocity (V_s) structure and geometry basin around Java Island. The result highlight low- V_s (1.7-22 km/s) corresponding to major basins such as Bogor, Banyumas and Kendeng Basins. Whereas the High V_s (2.3-3.2 km/s) observed in volcanic and basement rock region. West Java from cross-sections A-A' (Figure 11), illustrate northward-dipping basins which is Bogor Basins, with depths of 5–6 km inferred from the interpretation isolayer of V_s equal to 2.2 km/s. furthermore, these findings align with the tectonic role of the Baribis Fault in basin formation (Aribowo et al., 2022). Based on our result the present low V_s on the southern part of West Java at depth below 15 km could indicate the magmatism/basin that pass through the subduction process. Moving to Central and East Java, cross-section B-B' identifies the Banyumas basin through a prominent north-south-trending low- V_s , with the deepest low- V_s zone at its center, consistent with previews study about the existence of Banyumas basin (Setiawan et al., 2021). The vertical section further reveals two distinct low- V_s , the northern low V_s corresponds to the western margin of the Kendeng basin, while the southern anomaly reflects the eastern extent, supported by residual gravity anomaly models (Pohan et al., 2023). The Kendeng Basin illustrates in vertical-sections C-C, emerges as a continuous low- V_s structure extending from Central to East Java. The Sediment thicknesses of this basin reach 9–10 km (based on the interpretation of isolayer V_s equal to 2.2 km/s). In Addition,

215

220



225 validation of our interpretation from prior studies that attribute its formation to flexural subsidence linked to volcanic
arc loading and subduction dynamics (Martha et al., 2017; Novianto et al., 2020; Smyth et al., 2008).

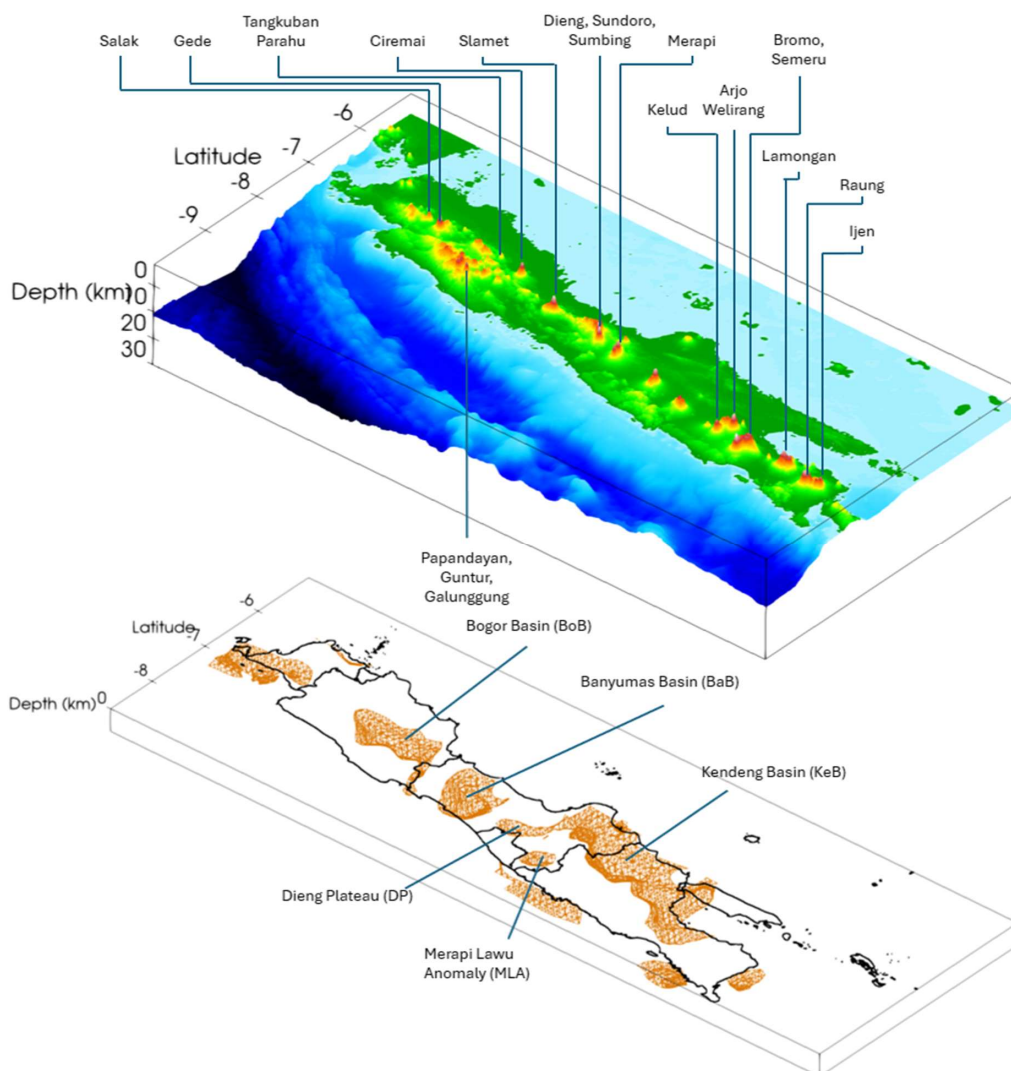


Figure 12: North-south section with 3D visualization of basins interpretation on isolayer of Vs equal to 2.2 km/s

Our results reveal a unique pattern of basin development along Java Island that reflects contrasting flexural responses
230 in the western and eastern domains. In western Java, the flexural trend displays northward basin development,
indicating that the lithosphere bends toward the north because of long-term subduction loading. The downward force
exerted near the southern margin associated with the slab and accretionary prism produces a foreland-style depression
that propagates northward. In contrast, eastern Java have different configuration in which the flexural axis shifts
southward. This southward orientation suggests a distinct mechanical coupling and stress regime between the
235 overriding Sunda Plate and the subducting slab, consistent with how the subduction system in this region has evolved



over geological time. Between these domains, central Java forms a transitional segment that accommodates the change in flexural geometry. The flexure here implies a twisting or rotational character, due to the **responds** in a non-uniform manner to spatially variable subduction-related forces. Overall, the contrasting flexural styles across the island align with the expected variations arising from the progressive tectonic development of the Java subduction system.

240

This rotational deformation may also reflect deep-seated structural segmentation within the Sunda Block; where pre-existing crustal weaknesses or fault systems influence the style of flexure. **The contrasting flexural trends from west to east thus highlight the mechanical heterogeneity of the Sunda Plate and suggest that subduction along Java is complex, uniform process but rather a dynamically evolving system governed by spatial variations in plate coupling, slab dip angle, and crustal properties.** Overall, the flexural pattern across Java Island provides important insight into the tectonic and mechanical response of the Sunda lithosphere to subduction. **It underscores the idea that Java's crustal deformation results from a combination of vertical bending due to slab loading and horizontal shearing due to oblique convergence, producing a complex interplay between flexural, rotational, and extensional processes along the island.**

245

4 Conclusion

250 This study presents the first crustal shear-wave velocity (V_s) **tomography** model encompassing the entire Java Island, derived from ambient seismic noise analysis. Utilizing data from 114 permanent seismograph stations (deployed in and outside Java Island) over a 6-month recording period, we compute more than 6,000 cross-correlation pairs and manually **picking** more than 5,000 dispersion curves to recover robust group velocity measurements across periods of 3–33 seconds and shear wave velocity from depth 3 to 29 km. Our model reveals the major basins across Java with clear evidence of depth structure. **The northern West Java, Bogor Basins exhibit low V_s value with basin thickness of 6 km illustrates from V_s value 1.3 to 2.2 km/s, aligning with their tectonic subsidence history influenced by the Baribis Fault system. Furthermore, in Central Java, the low V_s value (1.3–2.2 km/s) resolves the Banyumas Basin, highlighting their unique structural evolution under compressional back-arc tectonics.** Moreover, the Kendeng Basin is interpreted as a deep basin, continuous through extending across Central to East Java, revealing its flexural subsidence geometry with thicknesses exceeding 9–10 km in its central segment. Our regional interpretation about the contrasting flexural orientations between western and eastern Java suggests a large-scale twisting or rotational deformation of the island's crust, reflecting the differential response of the Sunda lithosphere to long-term subduction dynamics.

255

260

Author contribution: Iskandarsyah designed, carried out the data processing, interpretation, prepared the paper, Andri Dian Nugraha revised the paper, Zulfakriza Zulfakriza revised the paper, Irwan Meilano revised the paper, Bayu Pranata data provider and revise the paper, Samsul Hadi Wiyono revised the paper, Aditya Lesmana data processing and revised the paper, Rexha Verdhora, Ry revised the paper and plagiarism check, Muzli Muzli revised the plot result, Sesar Prabu Dwi data processing and plot visualization, Nova Heryandoko data processing and plot visualization revised the paper

270

Competing interests. The authors declare that they have no conflict of interest.



Code/Data availability. The shear-wave velocity (V_s) models, figures presented in this paper, and additional supporting images are available at Zenodo under DOI: <https://doi.org/10.5281/zenodo.17958206>

275 **5 Acknowledgments**

We gratefully acknowledge the Indonesian Agency for Meteorology, Climatology, and Geophysics (Badan Meteorologi, Klimatologi, dan Geofisika – BMKG) for providing critical seismic, geophysical, and monitoring datasets that underpinned this study. The high-quality seismic waveform data, station metadata, and tectonic monitoring records supplied by BMKG were indispensable for conducting ambient seismic noise tomography, shear-wave velocity modeling, and basin structural analyses. I sincerely thank Prof. Andri Dian Nugraha and Dr. Zulfakhriza
280 for providing me with the opportunity and support to carry out this research at ITB. An AI-assisted language editing tool was used to improve readability and grammar. The authors take full responsibility for the content of this manuscript.

References

- 285 Aribowo, S., Husson, L., Natawidjaja, D. H., Authemayou, C., Daryono, M. R., Puji, A. R., Valla, P. G., Pamumpuni, A., Wardhana, D. D., and de Gelder, G.: Active back-arc thrust in north west Java, Indonesia, *Tectonics*, 41, e2021TC007120, <https://doi.org/10.1029/2021TC007120>, 2022.
- Bensen, G., Ritzwoller, M., Barmin, M., Levshin, A. L., Lin, F., Moschetti, M., Shapiro, N., and Yang, Y.: Processing seismic ambient noise data to obtain reliable broad-band surface wave dispersion measurements, *Geophys. J. Int.*, 169, 1239–1260, <https://doi.org/10.1111/j.1365-246X.2007.03374.x>, 2007.
290
- Campillo, M. and Paul, A.: Long-range correlations in the diffuse seismic coda: *Science*, 2003.
- Doust, H. and Noble, R. A.: Petroleum systems of Indonesia, *Mar. Pet. Geol.*, 25, 103–129, <https://doi.org/10.1016/j.marpetgeo.2007.05.007>, 2008.
- Dziewonski, A., Bloch, S., and Landisman, M.: A technique for the analysis of transient seismic signals, *Bull. Seismol. Soc. Am.*, 59, 427–444, 1969.
295
- Hennino, R., Trégourès, N., Shapiro, N., Margerin, L., Campillo, M., Van Tiggelen, B., and Weaver, R.: Observation of equipartition of seismic waves, *Phys. Rev. Lett.*, 86, 3447, <https://doi.org/10.1103/PhysRevLett.86.3447>, 2001.
- Husein, S.: Petroleum and Regional Geology of Northeast Java Basin, Indonesia, *Int. Geol. Course Programme EXCURSION GUIDE BOOK Dec.*, 2015.
- 300 Irsyam, M., Cummins, P. R., Asrurifak, M., Faizal, L., Natawidjaja, D. H., Widiyantoro, S., Meilano, I., Triyoso, W., Rudiyanto, A., and Hidayati, S.: Development of the 2017 national seismic hazard maps of Indonesia, *Earthq. Spectra*, 36, 112–136, <https://doi.org/10.1177/8755293020951206>, 2020.
- Jiang, C. and Denolle, M. A.: NoisePy: A new high-performance python tool for ambient-noise seismology, *Seismol. Res. Lett.*, 91, 1853–1866, <https://doi.org/10.1785/0220190364>, 2020.
- 305 Kennett, B. L., Engdahl, E., and Buland, R.: Constraints on seismic velocities in the Earth from traveltimes, *Geophys. J. Int.*, 122, 108–124, 1995.



- Koulakov, I., Bohm, M., Asch, G., Lühr, B., Manzanares, A., Brotopuspito, K., Fauzi, P., Purbawinata, M., Puspito, N., and Ratdompurbo, A.: P and S velocity structure of the crust and the upper mantle beneath central Java from local tomography inversion, *J. Geophys. Res. Solid Earth*, 112, 2007a.
- 310 Koulakov, I., Bohm, M., Asch, G., Lühr, B., Manzanares, A., Brotopuspito, K., Fauzi, P., Purbawinata, M., Puspito, N., and Ratdompurbo, A.: P and S velocity structure of the crust and the upper mantle beneath central Java from local tomography inversion, *J. Geophys. Res. Solid Earth*, 112, <https://doi.org/10.1029/2006JB004712>, 2007b.
- Lesmana, A., Priyono, A., Nugraha, A. D., Rosalia, S., Sahara, D. P., Ry, R. V., Widiyantoro, S., Hidayat, W., Muttaqy, F., and Syahbana, D. K.: Revealing the shear-wave velocity structure of Tangkuban Parahu Volcano, West Java, Indonesia using Ambient Noise Tomography, *J. Volcanol. Geotherm. Res.*, 108371, <https://doi.org/10.1016/j.jvolgeores.2025.108371>, 2025.
- 315
- Lewis, J. P.: Fast normalized cross-correlation, *Vision interface*, 120–123, 1995.
- Martha, A. A., Cummins, P., Saygin, E., and Widiyantoro, S.: Imaging of upper crustal structure beneath East Java–Bali, Indonesia with ambient noise tomography, *Geosci. Lett.*, 4, 1–12, <https://doi.org/10.1186/s40562-017-0080-9>,
320 2017.
- Muttaqy, F., Nugraha, A. D., Mori, J., Puspito, N. T., Supendi, P., and Rohadi, S.: Seismic Imaging of Lithospheric Structure Beneath Central-East Java Region, Indonesia: Relation to Recent Earthquakes, *Front. Earth Sci.*, 10, 756806, <https://doi.org/10.3389/feart.2022.756806>, 2022.
- Noda, A.: Forearc basins: Types, geometries, and relationships to subduction zone dynamics, *Bulletin*, 128, 879–895, <https://doi.org/10.1130/B31345.1>, 2016.
325
- Novianto, A., Prasetyadi, C., Setiawan, T., and others: Structural model of Kendeng basin: a new concept of oil and gas exploration, *Open J. Yangtze Oil Gas*, 5, 200–215, <https://doi.org/10.4236/ojogas.2020.54016>, 2020.
- Pohan, A. F., Sismanto, S., Nurcahya, B. E., Lewerissa, R., Koesuma, S., Saputro, S. P., Amukti, R., Saputra, H., and Adhi, M. A.: Utilization and modeling of satellite gravity data for geohazard assessment in the Yogyakarta area of
330 Java Island, Indonesia, *Kuwait J. Sci.*, 50, 499–511, <https://doi.org/10.1016/j.kjs.2023.05.016>, 2023.
- Pranata, B., Yudistira, T., Widiyantoro, S., Brahmantyo, B., Cummins, P., Saygin, E., Zulfakriza, Z., Rosalia, S., and Cipta, A.: Shear wave velocity structure beneath Bandung basin, West Java, Indonesia from ambient noise tomography, *Geophys. J. Int.*, 220, 1045–1054, 2020.
- Ramdhan, M., Widiyantoro, S., Nugraha, A. D., Métaxian, J.-P., Rawlinson, N., Saepuloh, A., Kristyawan, S., Sembiring, A. S., Budi-Santoso, A., and Laurin, A.: Detailed seismic imaging of Merapi volcano, Indonesia, from local earthquake travel-time tomography, *J. Asian Earth Sci.*, 177, 134–145, <https://doi.org/10.1016/j.jseaes.2019.03.018>, 2019.
335
- Rawlinson, N.: FMST: fast marching surface tomography package–Instructions, *Res. Sch. Earth Sci. Aust. Natl. Univ. Canberra*, 29, 47, 2005.
- 340 Rosalia, S., Widiyantoro, S., Cummins, P. R., Yudistira, T., Nugraha, A. D., Zulfakriza, Z., and Setiawan, A.: Upper crustal shear-wave velocity structure Beneath Western Java, Indonesia from seismic ambient noise tomography, *Geosci. Lett.*, 9, 1–14, <https://doi.org/10.1186/s40562-021-00208-5>, 2022.
- Ry, R. V., Cummins, P. R., Hejrani, B., and Widiyantoro, S.: 3-D shallow shear velocity structure of the Jakarta Basin from transdimensional ambient noise tomography, *Geophys. J. Int.*, 234, 1916–1932,
345 <https://doi.org/10.1093/gji/ggad176>, 2023.



- Setiadi, T. A. P., Hartulistiyoso, E., Aidi, M. N., Martha, A. A., Daud, Y., Heryandoko, N., and Perdana, Y. H.: Identification of faults in the subsurface of Java Island using the ambient noise tomography method, *Mausam*, 76, 619–628, <https://doi.org/10.54302/mausam.v76i2.6195>, 2025.
- 350 Setiawan, A., Zulfakriza, Z., Nugraha, A. D., Rosalia, S., Priyono, A., Widiyantoro, S., Sahara, D. P., Marjiyono, M., Setiawan, J. H., and Lelono, E. B.: Delineation of sedimentary basin structure beneath the Banyumas Basin, Central Java, Indonesia, using ambient seismic noise tomography, *Geosci. Lett.*, 8, 1–15, <https://doi.org/10.1186/s40562-021-00202-x>, 2021.
- Shapiro, N. M., Campillo, M., Stehly, L., and Ritzwoller, M. H.: High-resolution surface-wave tomography from ambient seismic noise, *Science*, 307, 1615–1618, <https://doi.org/10.1126/science.1108339>, 2005.
- 355 Sigit, S.: *Geologic map of Indonesia-Peta geologi Indonesia*, US Geological Survey, 1965.
- Smyth, H. R., Hall, R., and Nichols, G. J.: Cenozoic volcanic arc history of East Java, Indonesia: the stratigraphic record of eruptions on an active continental margin, [https://doi.org/10.1130/2008.2436\(10\)](https://doi.org/10.1130/2008.2436(10)), 2008.
- Steinshouer, D. W., Qiang, J., McCabe, P. J., and Ryder, R. T.: *Maps showing geology, oil and gas fields, and geologic provinces of the Asia Pacific region*, US Geological Survey, 1999.
- 360 Syaifuddin, F., Zulfakriza, Nugraha, A. D., and Daryono, M. R.: Spatial variations of shear-wave velocity anomaly derived from Love wave ambient noise seismic tomography along Lembang Fault (West Java, Indonesia), *Open Geosci.*, 17, 20220665, <https://doi.org/10.1515/geo-2022-0665>, 2025.
- Tian, Y. and Ritzwoller, M. H.: Directionality of ambient noise on the Juan de Fuca plate: implications for source locations of the primary and secondary microseisms, *Geophys. J. Int.*, 201, 429–443, <https://doi.org/10.1093/gji/ggv024>, 2015.
- 365 <https://doi.org/10.1093/gji/ggv024>, 2015.
- Varotsos, P. K. and Sarlis, N. V.: Green's Function, Earthquakes, and a Fast Ambient Noise Tomography Methodology, *Appl. Sci.*, 14, 697, <https://doi.org/10.3390/app14020697>, 2024.
- Wagner, D., Koulakov, I., Rabbal, W., Luehr, B.-G., Wittwer, A., Kopp, H., Bohm, M., Asch, G., and MERAMEX scientists: Joint inversion of active and passive seismic data in Central Java, *Geophys. J. Int.*, 170, 923–932, <https://doi.org/10.1111/j.1365-246X.2007.03435.x>, 2007.
- 370 <https://doi.org/10.1111/j.1365-246X.2007.03435.x>, 2007.
- Widiyantoro, S., Pesicek, J., and Thurber, C.: Subducting slab structure below the eastern Sunda arc inferred from non-linear seismic tomographic imaging, <https://doi.org/10.1144/SP355.7>, 2011.
- Yang, Y., Ritzwoller, M. H., Levshin, A. L., and Shapiro, N. M.: Ambient noise Rayleigh wave tomography across Europe, *Geophys. J. Int.*, 168, 259–274, 2007.
- 375 Zulfakriza, Saygin, E., Cummins, P., Widiyantoro, S., and Nugraha, A. D.: Upper crustal structures beneath Yogyakarta imaged by ambient seismic noise tomography, *AIP Conference Proceedings*, 269–272, 2013.